

Structure of ^{20}Ne : The $^{19}\text{F}(^3\text{He}, d)^{20}\text{Ne}$ reaction*

R. R. Betts,[†] H. T. Fortune, and R. Middleton

Physics Department, University of Pennsylvania, Philadelphia, Pennsylvania 19174

(Received 8 July 1974)

The $^{19}\text{F}(^3\text{He}, d)^{20}\text{Ne}$ reaction has been studied at a bombarding energy of 18 MeV. Levels were identified up to an excitation energy of 13.3 MeV in ^{20}Ne . Several new spin-parity and isospin assignments are made. A comparison of the experimental spectroscopic strengths with those predicted by the Nilsson, SU(3), and shell models shows reasonably good agreement.

[NUCLEAR REACTIONS $^{19}\text{F}(^3\text{He}, d)$, $E = 18$ MeV; measured $\sigma(E_d, \theta)$; ^{20}Ne deduced] levels, l , J , π , T .

I. INTRODUCTION

The nucleus ^{20}Ne is one of the best examples of a light deformed nucleus,¹ and has been firmly established as such for some time. Interpretations of the level structure of ^{20}Ne in terms of the Nilsson model² and in terms of the SU(3) classification of the shell model^{3,4} have been reasonably successful. The known rotational structures in ^{20}Ne have been extended to quite high spins.⁵⁻⁸

Recently, many-particle shell-model calculations⁹⁻¹¹ for ^{20}Ne have been able to reproduce many of the "collective" features of this nucleus. It therefore provides a unique meeting point between the collective models of nuclear structure and the more general (although more cumbersome) shell-model approach.

A wealth of experimental information exists on the properties of ^{20}Ne . Most of these results are included in the recent $A = 18-20$ compilation of Ajzenberg-Selove.¹²

The present paper forms the first of a series of reports on the experimental investigation of ^{20}Ne using single- and multi-nucleon transfer reactions, and concerns the $^{19}\text{F}(^3\text{He}, d)^{20}\text{Ne}$ reaction.

Previous studies of proton stripping reactions leading to ^{20}Ne include work on the $^{19}\text{F}(^3\text{He}, d)$, $^{19}\text{F}(\alpha, t)$, and $^{19}\text{F}(d, n)$ reactions.^{2, 13-17} In the main, however, these investigations have presented only a limited set of results. The present work consists of a high-resolution study of the excitation range 4-13 MeV, and therefore represents a more complete set of results than those of the previous workers.

II. EXPERIMENTAL PROCEDURES

A beam of 18-MeV $^3\text{He}^{++}$ ions from the University of Pennsylvania tandem Van de Graaff was used to bombard a calcium fluoride target placed

in the multiangle spectrograph. The target consisted of a layer of calcium fluoride enriched to 99.97% in ^{40}Ca evaporated onto a $75\text{-}\mu\text{g}/\text{cm}^2$ gold backing. The choice of target was dictated by the desire to minimize the yield of contaminant groups in the deuteron spectrum. The target thickness was obtained by measuring the yield of elastically scattered beam particles from the ^{40}Ca (observed in a silicon surface-barrier detector mounted at $33\frac{3}{4}^\circ$ to the beam direction) and comparing it to the cross section previously measured at this energy by Abdo.¹⁸ This procedure gave the thickness of the ^{40}Ca which, together with the assumption of two fluorine atoms for each calcium atom, then gave the ^{19}F thickness of $27\ \mu\text{g}/\text{cm}^2$. The condition of the target was monitored continuously throughout the experiment; no deterioration was observed. The reaction deuterons were recorded on Ilford K2 nuclear emulsions mounted in the focal planes of the spectrograph. Suitably chosen foils stopped α particles and ^3He particles from striking the emulsions.

III. RESULTS AND ANALYSIS

A spectrum measured at $7\frac{1}{2}^\circ$ covering the excitation range 4-9.5 MeV is shown in Fig. 1. The ^{20}Ne levels are identified by their excitation energies. The measured width of the 5.785-MeV level is 23 keV. Since this level is known¹² to have a very small natural width the above number is therefore indicative of the experimental resolution. Figure 2 shows the spectrum of the excitation range 9.5-13.5 MeV and is plotted on an expanded horizontal scale. Again, ^{20}Ne levels are identified by their excitation energies and groups arising from the $(^3\text{He}, d)$ reaction on the ^{40}Ca , ^{12}C , and ^{16}O contaminants are labeled by the final nucleus and level number. The extremely low background in both spectra is notable, thus enabling the positive iden-

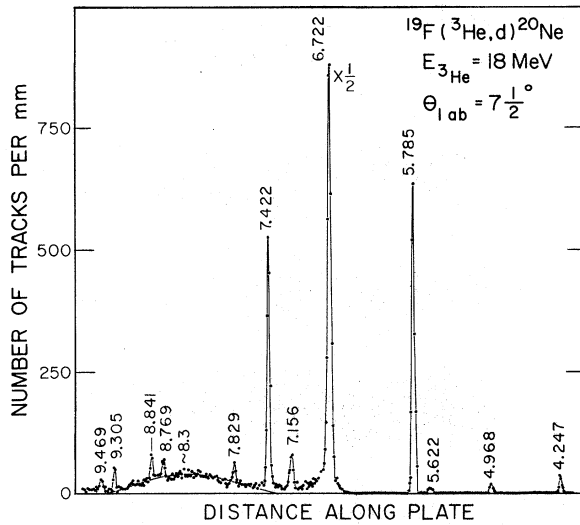


FIG. 1. Spectrum of the $^{19}\text{F}(^3\text{He},d)^{20}\text{Ne}$ reaction covering the excitation range 4–9.5 MeV.

tification of several quite broad groups.

Excitation energies of the ^{20}Ne levels were calculated using the known magnet calibration and the exact beam energy calculated from the positions of the strong contaminant peaks. Resulting excitation energies are listed in Table I. Uncertainties in the excitation energies are about 3 keV for the strong states below 10 MeV in excitation, and 6–10 keV for the weak states in that region. Above 10 MeV, our excitation energies are internally consistent to within about 4 keV for most states. However, due to the possibility of systematic errors, we quote an uncertainty of ± 15 keV for states above 10 MeV. The presence of rather large discrepan-

cies, for some states, between our excitation energies and those in the recent compilation¹² is disturbing, but we offer no explanation.

Additionally, widths were obtained for several groups by direct measurement of the spectra; the contribution of the experimental resolution to the width was subtracted quadratically. The natural widths thus obtained are also listed in Table I.

Angular distributions were extracted for transitions to all the labeled states and are shown in Figs. 3 and 4. The absolute cross-section scale was determined using the measured target thickness and collected charge and is believed accurate to within 15%.

A distorted-wave analysis of the angular distributions was performed using the code DWUCK.¹⁹ The optical-model and bound state parameters were taken from other work in this mass region^{20,21} and are listed in Table II. The results of the distorted-wave calculations are shown superimposed on the data in Figs. 3 and 4.

The relation between the measured and calculated cross sections for the $(^3\text{He},d)$ reaction on a $J = \frac{1}{2}$, $T = T_z = \frac{1}{2}$ nucleus is

$$\sigma_{\text{exp}}(\theta) = 1.105(2J_f + 1) \sum_{nlj} S_{nlj} \frac{\sigma_{nlj}(\theta)}{2j + 1},$$

where J_f is the spin of the final state and j is the transferred total angular momentum. The above relation was used to calculate spectroscopic strengths $[(2J_f + 1)S_{nlj}]$ for those transitions characteristic of direct stripping. These strengths are also given in Table I. The present spectroscopic factors are in rather poor agreement with those of Ref. 2 but are in good agreement with the more recent measurements of Obst and Kemper.¹⁷

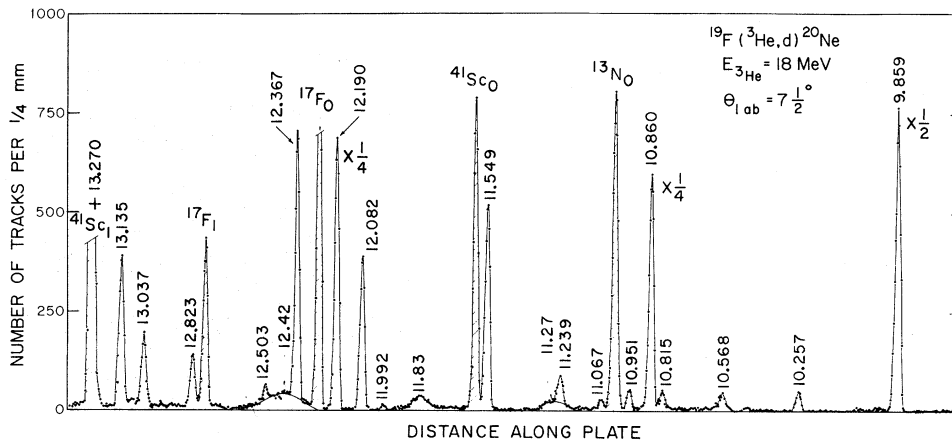


FIG. 2. Spectrum of the $^{19}\text{F}(^3\text{He},d)^{20}\text{Ne}$ reaction covering the excitation range 9.5–13.5 MeV.

TABLE I. Results of the $^{19}\text{F}(^3\text{He}, d)^{20}\text{Ne}$ reaction.

| Present work | | | | Literature ^a | | | Comments |
|---------------------|-------------------|--|--|-------------------------|-------------------|--------------|---|
| E_x (MeV) | Γ (keV) | nlj | $(2J_f + 1)S$ | E_x (MeV) | Γ (keV) | J^π | |
| 4.247 | | n.s. | ... | 4.247 | | 4^+ | |
| 4.967 | | $(2p_{3/2})$ | 0.03 | 4.968 | | 2^- | |
| 5.622 | | $(1f_{7/2})$ | 0.09 | 5.622 | | 3^- | |
| 5.785 | | $2p_{3/2}$ | 0.16 | 5.785 | | 1^- | |
| 6.722 | | $2s_{1/2}$ | 0.52 | 6.722 | | 0^+ | |
| 7.156 | | $1f_{7/2}$ | 0.42 | 7.166 | 8 | 3^- | |
| 7.422 | | $1d_{5/2}$ | 0.79 | 7.424 | 8 | 2^+ | |
| 7.829 | | $1d_{5/2}$ | 0.06 | 7.834 | 2 | 2^+ | |
| ~8.3 | ~800 | $2s_{1/2}$ | 0.13 | ~8.6 | >800 | 0^+ | |
| 8.769 | | n.s. | ... | 8.775 | | 6^+ | |
| 8.841 | | $(2p_{3/2})$ | 0.01 | 8.850 | 19 | 1^- | |
| 9.305 | | $1d_{5/2}$ | 0.04 | (9.34) | | | $(1, 2, 3)^+$ |
| 9.469 | | $1d_{5/2}$ | 0.03 | 9.489 | 29 | 2^+ | |
| 9.859 | | $1d_{5/2}$ | 2.37 | 9.87 | | | $3^+(1, 2)^+$ |
| 10.257 | | $1d_{5/2}$ | 0.07 | 10.26 | ≤ 2 | $2^+, T=1$ | |
| 10.568 | 27 | $1d_{5/2}$ | 0.05 | 10.579 | 24 | 2^+ | |
| 10.815 | 12 | $1d_{5/2}$ | 0.05 | 10.836 | 13 | 2^+ | |
| 10.860 | | $1d_{5/2}$ | 2.82 | 10.853 | | $(2^+), T=1$ | $3^+, T=2$ |
| 10.951 | | | | | | | |
| 11.067 | | n.s. | ... | 11.08 | | $(4^+, T=1)$ | |
| 11.239 | | $\left\{ \begin{array}{l} 2s_{1/2} \\ 2p_{3/2} \\ 1d_{3/2} \end{array} \right\}$ | $\left\{ \begin{array}{l} 0.02 \\ 0.02 \\ 0.03 \end{array} \right\}$ | 11.233 | | $(1^+, T=1)$ | $(1^+, T=1$ and $1^-, T=1$ doublet) |
| 11.27 | 73 | n.s. | ... | 11.324 | 53 | 2^+ | |
| 11.549 | | $1d_{5/2}$ | 1.00 | 11.549 | | $(T=1)$ | $3^+(1, 2)^+, T=0$ |
| 11.83 | 81 | $1d_{5/2}$ | 0.10 | 11.871 | 46 | 2^+ | |
| 11.992 | | n.s. | ... | | | | $(T=1?)$ |
| 12.082 | | $1d_{5/2}$ | 0.35 | 12.086 | | $(T=1)$ | $3^+(1, 2)^+$ |
| 12.190 | | $1d_{5/2}$ | 2.10 | (12.200) | | $(T=1)$ | $2^+, T=1$ |
| 12.367 | | $\left\{ \begin{array}{l} 2s_{1/2} \\ 1d_{3/2} \end{array} \right\}$ | $\left\{ \begin{array}{l} 0.37 \\ 0.19 \end{array} \right\}$ | | | | 1^+ |
| 12.423 | 160 | $1d_{5/2}$ | 0.19 | | | | $2^+(1, 3)^+$ |
| 12.503 | | $1d_{5/2}$ | 0.02 | | | | $(1^+, 2^+, 3^+)$ |
| 12.823 | | $2s_{1/2}$ | 0.15 | | | | 1^+ |
| 13.037 | | $1d_{5/2}$ | | | | | $(1, 2, 3)^+$ |
| 13.135 ^b | | $\left\{ \begin{array}{l} 2s_{1/2} \\ 1d_{5/2} \end{array} \right\}$ | | | | | 1^+ |
| 13.270 ^b | | | | | | | |

^a Reference 12.^b Proton unbound.TABLE II. Optical-model parameters used in the distorted-wave analysis of the $^{19}\text{F}(^3\text{He}, d)^{20}\text{Ne}$ reaction.

| Channel | V_0 (MeV) | $r_0=r_{s0}$ (fm) | $a=a_{s0}$ (fm) | W (MeV) | $W'=4W_D$ (MeV) | r'_0 (fm) | a' (fm) | r_{0c} (fm) | V_{s0} (MeV) |
|--|----------------|----------------------|--------------------|--------------|--------------------|----------------|--------------|------------------|-------------------|
| $^{19}\text{F} + ^3\text{He}$ ^a | 177.0 | 1.14 | 0.72 | 13.0 | ... | 1.60 | 0.77 | 1.40 | 8.0 |
| $^{20}\text{Ne} + d$ ^a | 105.0 | 1.02 | 0.86 | ... | 80.0 | 1.42 | 0.65 | 1.02 | 6.0 |
| Bound state ^b | c | 1.26 | 0.60 | ... | ... | ... | ... | ... | $\lambda=25$ |

^a Reference 20.^b Reference 21.^c Adjusted to give the correct binding energy as determined by the separation energy procedure.

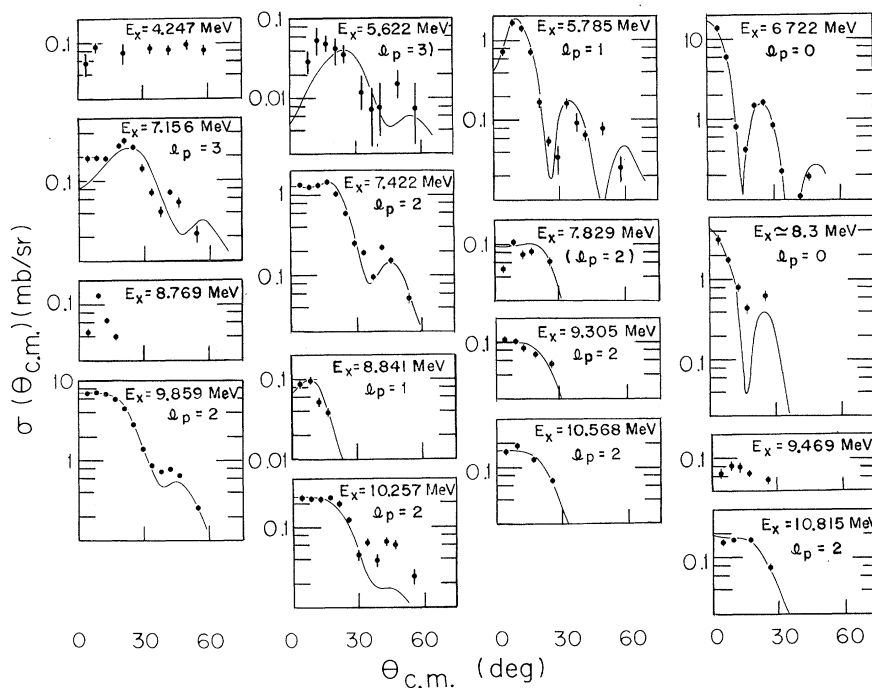


FIG. 3. Angular distributions of $^{19}\text{F}(^3\text{He}, d)^{20}\text{Ne}$ transitions. The curves are the results of distorted-wave calculations.

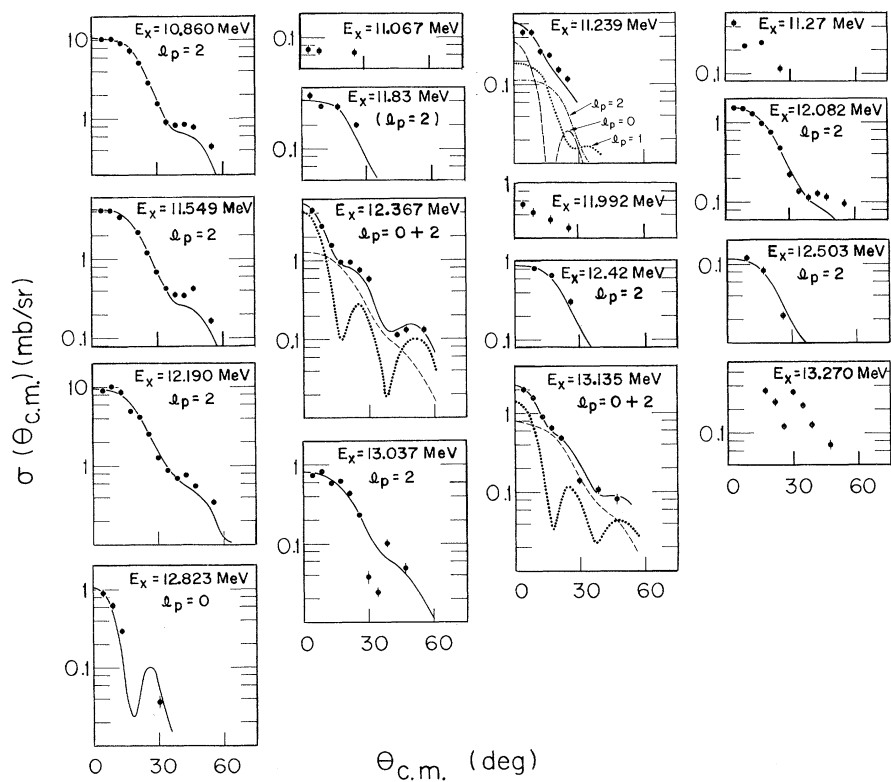


FIG. 4. Angular distributions of $^{19}\text{F}(^3\text{He}, d)^{20}\text{Ne}$ transitions. The curves are the results of distorted-wave calculations.

IV. COMPARISON WITH PREVIOUS RESULTS AND SPIN ASSIGNMENTS

Most of the relevant information on the ^{20}Ne level scheme is summarized in the recent compilation of Ajzenberg-Selove.¹² In most cases it is possible to associate the levels observed in the present work with those previously reported, although in a few cases the agreement between the energies is rather poor. In several cases we are able to make new spin-parity assignments based on the selection rules of the $(^3\text{He}, d)$ reaction on a $J^\pi = \frac{1}{2}^+$ target.

Before discussing the individual levels, however, there are some general comments which hold for all transitions. ^{20}Ne becomes unbound to α -particle emission to the ^{16}O ground state at an excitation energy of 4.730 MeV, and many of the levels above this excitation energy have a significant natural width. Those states with no natural width should therefore fall into one or more of the following categories:

- (i) Those with unnatural parity [$\pi = -(-1)^J$]. The angular momentum and parity conservation rules forbid the α decay of such states to the ^{16}O ground state. This restriction is no longer valid above $E_x = 10.361$ MeV since α decay to the 6.131-MeV, $J^\pi = 3^-$ state in ^{16}O then becomes energetically possible.
- (ii) Those with $T > 0$. Below $E_x = 12.845$ MeV (the $^{19}\text{F} + p$ threshold) only $T = 0 \rightarrow T = 0$ decays are energetically possible. If, therefore, we regard isospin as a good quantum number, $T \geq 1$ states in ^{20}Ne should have no natural width. Above $E_x = 12.845$ MeV, proton decays to the ^{19}F ground state are allowed, thus permitting $T = 1$ states to have natural width.
- (iii) Those with small reduced widths. It is, of course, possible for an energetically allowed decay to be inhibited for structural or kinematical reasons. In such cases, the lack of natural width cannot be taken to imply either of the above two possibilities. We will, however, assume possibilities (i) and (ii) to be more probable whilst not excluding possibility (iii).

We turn now to a state-by-state discussion of the results. The level observed at 4.247 MeV is known to have spin-parity 4^+ and has been placed in the ground-state rotational band.¹ The angular distribution observed for the transition to this state is not characteristic of direct stripping. This result is not unexpected in view of the known structure of this band, which consists largely of four $2s-1d$ shell nucleons outside a closed ^{16}O core. Its strength, however, is somewhat surprising. The population of this state must involve processes of higher order than simple direct one-step stripping. Further discussion of this point is beyond the scope

of this paper, and it has previously been covered in detail in Ref. 17. Similar comments apply to the level observed at 8.769 MeV which corresponds to the 6^+ member of the ground-state band.

Both the 4.968-MeV (2^-) and 5.622-MeV (3^-) members of the $K^\pi = 2^-$ band are weakly populated, although the angular distribution of the latter transition does bear some resemblance to an $l_p = 3$ distorted-wave calculation. The 4.968-MeV state is relatively strongly populated in the $^{21}\text{Ne}(^3\text{He}, \alpha)^{20}\text{Ne}$ reaction.²² Both these results are consistent with the proposed structure of this band as arising from the coupling of five $2s-1d$ shell nucleons to a hole in the $1p$ shell.

The lowest-lying negative-parity band based on the excitation of a particle is expected to be composed of three nucleons in the $2s-1d$ shell and one in the $1f-2p$ shell. The strong $l_p = 1$ transition to the 5.785-MeV (1^-) level agrees with this interpretation, as does the $l_p = 3$ transition to the 7.156-MeV (3^-) member of this $K^\pi = 0^-$ band. Further discussion of the strengths of these transitions will be given in the next section.

For the first excited $K^\pi = 0^+$ band, both the 0^+ and 2^+ members, at 6.722 and 7.422 MeV, respectively, are strongly excited in this reaction. The 7.196-MeV (0^+) and 7.829-MeV (2^+) members of a neighboring $K^\pi = 0^+$ band on the other hand, are only very weakly excited. In fact, the 7.196-MeV state is completely absent and the angular distribution of the 7.829-MeV state is not particularly characteristic of direct stripping. This result is consistent with the proposed structure²³ of these two bands—the first arising from dominantly $2s-1d$ shell configurations and the second from excitations out of an ^{16}O core.

The strong excitation of the broad ($\Gamma = 800$ keV) 0^+ state near 8.3 MeV excitation is quite remarkable. The angular distribution is well accounted for by an $l_p = 0$ distorted-wave calculation and the spectroscopic strength is relatively large—0.13, to be compared with a strength of 0.52 for the 6.722-MeV state. This result has been interpreted²⁴ as due to the mixing of a dominantly $2s-1d$ shell state (which has a large single-particle spectroscopic strength) and a state with at least two $1f-2p$ shell particles (which has a large α width). Mixing of these two states was then able²⁴ to explain the single-particle spectroscopic factors and α widths of the 6.722- and 8.3-MeV states.

Weak transitions are observed to levels at 8.841 MeV (8.850 MeV, $J^\pi = 1^-$), 9.305 MeV (9.34 MeV), and 9.469 MeV (9.489 MeV, $J^\pi = 2^+$), where the energies and spins in parenthesis refer to those in the compilation.¹²

No mention is made of any level near 9.859 MeV in the recent compilation,¹² although Ritter, Par-

son, and Bernard,¹⁶ in their study of the $^{19}\text{F}(d, n)^{20}\text{Ne}$ reaction, reported the existence of a level at 9.87 MeV, which most probably corresponds to the level observed in the present work. The angular distribution of this transition is unambiguously characteristic of $l_p = 2$ transfer, and the group has no measurable width. The $l_p = 2$ transition requires $J^\pi = 1^+, 2^+, \text{ or } 3^+$. The absence of any natural width would tend to exclude the 2^+ possibility, and the failure to detect any $l_p = 0$ component in the angular distribution would seem to make 1^+ unlikely. We therefore favor a 3^+ assignment for this level with 1^+ and 2^+ not entirely ruled out.

The level observed at 10.257 MeV corresponds to the lowest $T = 1$ level in ^{20}Ne which has a spin-parity of 2^+ . Although this level is only weakly excited, the angular distribution is well accounted for by an $l_p = 2$ calculation, consistent with the known spin and parity. Additionally, the measured spectroscopic strength in the present work is 0.07, in excellent agreement with that measured in the $^{19}\text{F}(d, p)$ reaction²⁵ to the ground state of ^{20}F : $(2J_f + 1)S \approx 0.06$. This result is consistent with the expectations for analog transitions.

The 10.568-MeV level observed in the present work has a measured width of 27 keV, in good agreement with the previously reported value of 24 keV.¹² The angular distribution is fairly well accounted for by an $l_p = 2$ calculation, consistent with the accepted spin-parity of 2^+ and $T = 0$. Similarly, the measured width of 12 keV and the $l_p = 2$ angular distribution for the 10.815-MeV state are also consistent with the width (13 keV) and spin-parity (2^+) of a state at $E_x = 10.836$ MeV from earlier work.¹²

The strong $l_p = 2$ transition observed for the level at $E_x = 10.860$ MeV is in agreement with the expectations for the $J^\pi = 3^+, T = 1$ analog of the 0.656-MeV, $J^\pi = 3^+$ ^{20}F state. The spectroscopic strengths from the present work and the previous $^{19}\text{F}(d, p)^{20}\text{F}$ study²⁵ are 2.82 and 2.59, respectively, further strengthening this belief. The 3^+ assignment for this state thus appears firm, replacing the (2^+) assignment from the compilation.¹²

The 11.067-MeV state has previously been assigned $J^\pi = 4^+, T = 1$, the analog of the 0.823-MeV ^{20}F second excited state. This level is only weakly populated in the present study, and the angular distribution is not characteristic of direct stripping. This result is consistent with that obtained for the $^{19}\text{F}(d, p)^{20}\text{F}$ transition to the 0.823-MeV level.^{25, 26}

Two states are observed near 11.3 MeV in excitation, at 11.239 and 11.27 MeV, respectively. The analogs of the 0.984-MeV ($J^\pi = 1^-$) and 1.057-MeV ($J^\pi = 1^+$) ^{20}F states^{12, 25} are expected to occur in this excitation range. Of the two levels observed

in the present work, the state at 11.27 MeV can be excluded as a possible $T = 1$ state, since it has a large (73-keV) width. This state most probably corresponds to the $J^\pi = 2^+$ state at 11.324 MeV reported in the compilation which has a width of 53 keV. The level observed at 11.239 MeV has no measurable width and although its angular distribution is not particularly characteristic of a single l_p value, the shape is well accounted for by an admixture of $l_p = 0$ and 2. This procedure gives nearly the same spectroscopic strengths as obtained for the 1.057-MeV ^{20}F state in the $^{19}\text{F}(d, p)$ reaction.²⁶ This result is consistent with the J^π value of 1^+ noted in Ref. 12. There is no candidate for the analog of the 0.984-MeV ($J^\pi = 1^-$) level. However, the expected strength of such a transition is within the sensitivity of the present study if it is resolved from other states, and it is surprising that no other level in ^{20}Ne is seen to be excited in this excitation range. We therefore propose that the 11.239-MeV level is in fact a closely spaced doublet with $J^\pi = 1^+, T = 1$ and $J^\pi = 1^-, T = 1$ members. Assuming this, we include an $l_p = 1$ contribution in the fit to the experimental shape of this transition which is shown in Fig. 4. The spectroscopic strengths extracted using this procedure show good agreement with the (d, p) results.²⁶ A study of the $^{21}\text{Ne}(^3\text{He}, \alpha)^{20}\text{Ne}$ reaction should enable the positive identification of the analog of the 0.984-MeV ^{20}F level as this level is seen to be strongly excited in the $^{21}\text{Ne}(d, ^3\text{He})^{20}\text{F}$ reaction.²⁷

The next $T = 1$ level expected in ^{20}Ne is the analog of the 1.309-MeV $J^\pi = 2^-$ state in ^{20}F and should be near 11.5 MeV in ^{20}Ne . This level is only weakly populated in the $^{19}\text{F}(d, p)^{20}\text{F}$ reaction^{25, 26} and it is therefore expected that the analog transition will be correspondingly weak. No weak transitions are observed in the present study near 11.5 MeV excitation; however, it is possible that such a level is obscured by the strong contaminant group corresponding to the ^{41}Sc ground state. As in the case of the 0.984-MeV ($J^\pi = 1^-$) ^{20}F level, the 1.309-MeV ^{20}F level is strongly excited in the $^{21}\text{Ne}(d, ^3\text{He})^{20}\text{F}$ reaction²⁷ and the analog should therefore easily be identified in the $^{21}\text{Ne}(^3\text{He}, \alpha)^{20}\text{Ne}$ reaction.

The level at 11.549 MeV has previously been suggested to have $T = 1$ on the basis of its strong excitation in the $^{19}\text{F}(d, n)^{20}\text{Ne}$ reaction.¹⁵ As in previous work, the present study shows a relatively strong $l_p = 2$ transition to this level, and the group has no measurable natural width. There is however, no corresponding level in ^{20}F with the correct parity, and we therefore tentatively rule out the possibility of $T = 1$ character for this level. Arguments similar to those for the 9.857-MeV level lead to a suggested assignment of $J^\pi = 3^+$ with $J^\pi = 1^+$ on 2^+ not entirely excluded.

A broad ($\Gamma=81$ -keV) state is observed at 11.83 MeV. This state probably corresponds to the $J^\pi=2^+$ state observed²⁸ as a resonance in α scattering on ^{16}O at $E_x(^{20}\text{Ne})=11.87\pm 0.02$ MeV with a width of 46 keV. The apparent $l_p=2$ angular distribution is consistent with the supposed spin-parity of 2^+ .

The transition to the level at 12.082 MeV has a strong $l_p=2$ angular distribution. This state has been previously suggested to have $T=1$ character, but the strength observed in the present study [$(2J_f+1)S=0.35$] is too large for it to be associated with any ^{20}F state in the correct excitation range. We therefore favor a 3^+ , $T=0$ assignment with 1^+ and 2^+ not excluded, on the same grounds as for the 9.859- and 11.549-MeV transitions.

The weak transition to the level at 11.992 MeV, although not characteristic of direct stripping, has about the right strength to be the analog of either or both of the 1.824- or 1.843-MeV ^{20}F states. We therefore tentatively suggest a $T=1$ assignment for the 11.992-MeV level.

A state at 12.200 MeV has been tentatively identified as having $T=1$ character. This state probably corresponds to the level observed at 12.190 MeV in the present work. The angular distribution is well accounted for by an $l_p=2$ calculation, and the strength [$(2J_f+1)S=2.10$] agrees well with that measured²⁵ for the $^{19}\text{F}(d, p)$ transition to the 2.044-MeV ($J^\pi=2^+$) ^{20}F state which has a spectroscopic strength of 2.32. The previous suggestion of $T=1$ character for the 12.190-MeV state is therefore confirmed and a spin-parity of 2^+ assigned.

The $l_p=0+2$ transition to the 12.367-MeV level enables an unambiguous assignment of $J^\pi=1^+$. It is probable that this state has $T=0$ since no known ^{20}F state near $E_x=2.1$ MeV has $J^\pi=1^+$.

An $l_p=2$ transition to the 12.423-MeV level requires $J^\pi=(1, 2, 3)^+$. The width of this group ($\Gamma=160$ keV) would suggest natural parity, although

TABLE III. Comparison of $^{19}\text{F}(d, p)$ and $^{19}\text{F}(^3\text{He}, d)$ spectroscopic strengths for $T=1$ states.

| $^{19}\text{F}(d, p)^{20}\text{F}$ ^a | | | $^{19}\text{F}(^3\text{He}, d)^{20}\text{Ne}$ ^b | |
|---|---|---------|--|--|
| E_x (^{20}F) (MeV) | $(2J_f+1)S$ | J^π | E_x (^{20}Ne) (MeV) | $(2J_f+1)S$ |
| 0 | ≤ 0.06 | 2^+ | 10.257 | 0.07 |
| 0.656 | 2.59 | 3^+ | 10.860 | 2.82 |
| 0.823 | ≤ 0.03 | 4^+ | (11.067 | n.s.) |
| 0.983 | | 1^- | (11.239 | 0.02) |
| 1.056 | $\left\{ \begin{array}{l} 0.02 \\ \leq 0.03 \end{array} \right\}$ | 1^+ | (11.239 | $\left\{ \begin{array}{l} 0.02 \\ 0.03 \end{array} \right\}$ |
| 2.044 | 2.32 | 2^+ | 12.190 | 2.10 |

^a References 25 and 26.

^b Present work.

α decay to the 6.131-MeV ^{16}O $J^\pi=3^-$ level is allowed with an α energy of 1.5 MeV, thus permitting a 1^+ or 3^+ state to have natural width. Thus, we favor the $J^\pi=2^+$ possibility whilst not excluding 1^+ or 3^+ . Similarly, we observe an $l_p=2$ transition to the 12.503-MeV level, which has no natural width. Its spin-parity is thus $(1, 2, 3)^+$.

The $l_p=0$ transition to the 12.823-MeV state requires $J^\pi=0^+$ or 1^+ . The fact that no state near 2.5 MeV in ^{20}F is populated with $l_p=0$ in the $^{19}\text{F}(d, p)^{20}\text{F}$ reaction leads to a $T=0$ assignment and the lack of natural width would appear to rule out the 0^+ possibility.

Above $E_x=12.845$ MeV, ^{20}Ne is unbound to proton emission. Conventional distorted-wave Born-approximation (DWBA) techniques therefore do not permit the reliable extraction of spectroscopic information. They will, however, still give an adequate description of the angular distribution shapes if a bound form factor is used. Correct DWBA calculations for these and higher unbound states are in progress. The angular distributions of the 13.037- and 13.135-MeV transitions are well fitted by $l_p=2$ and $l_p=0+2$ calculations, respectively. The latter enables a firm $J^\pi=1^+$ assignment for the 13.135-MeV level.

The results discussed in this section are summarized in Table I. For $T=1$ levels, the comparison with the (d, p) results is given in Table III, and Fig. 5 shows these levels together with the ^{20}F level scheme.

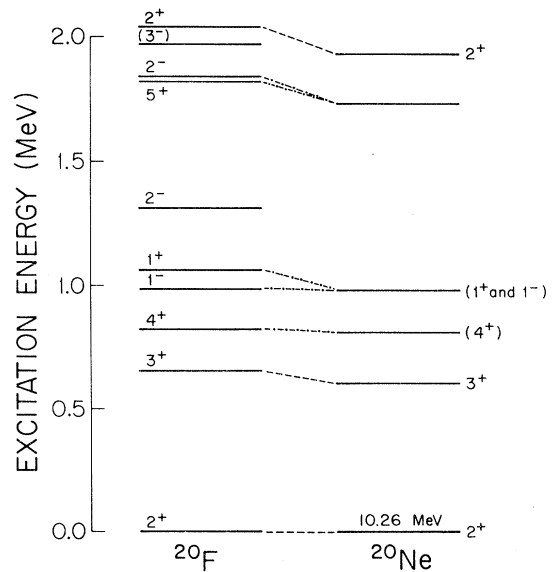


FIG. 5. Comparison of the ^{20}F level scheme with previously known and proposed $T=1$ levels in ^{20}Ne . Firm correspondences are indicated by dashed (---) lines. Tentative correspondences are shown with dash-dotted (-.-.) lines.

V. COMPARISON WITH MODEL CALCULATIONS

As discussed in the Introduction, the nucleus ^{20}Ne is one of the few light deformed nuclei for which detailed shell-model calculations exist. It is therefore interesting to compare the results of these two different approaches (viz. large basis shell-model calculations and deformed models) with the present experimental results.

Before embarking on a critical discussion of the successes and failures of these two approaches it is worthwhile to make some general observations that will indicate the scope of the problem. It is clear from the present experimental results that most of the levels observed can be described as arising from $2s$ - $1d$ shell configurations. The dominance of $l_p=0$ and 2 transitions shows this, although the available strength is by no means exhausted. On the other hand, significant amounts of $l_p=1$ and 3 strength are observed at relatively low excitation energies thus indicating the importance of $1f$ - $2p$ shell orbitals. Finally, it is known, though not from the present data, that $1p$ -shell hole configurations are also very important at low excitations in ^{20}Ne . These observations are relatively easily interpreted in the framework of the Nilsson model. For large deformations, the notion of spherical shell closures largely disappears, thus allowing configurations from different major shells to be quite close in energy. Detailed shell-model calculations are largely unable to explain these results, although this is probably due solely to the necessary truncations involved in these types of calculations.

Collective models

The unified model has been very successful in explaining many of the properties of nuclei in this mass region. In this picture, the ^{19}F ground state is described as three nucleons in Nilsson orbit No. 6, $\frac{1}{2}^+[220]$. The two lowest $K^\pi=0^+$ bands in ^{20}Ne are then formed by adding a proton to either this orbit (ground state) or to orbit No. 9, $\frac{1}{2}^+[211]$ (the 0^+ state at 6.72 MeV). Spectroscopic strengths expected for the 0^+ and 2^+ members of these bands were calculated using Satchler's formula,²⁹ and Chi's tabulation³⁰ of Nilsson wave functions. These strengths are shown plotted as a function of deformation (δ) in Fig. 5, together with the data for the ground-state, 1.63-, 6.72-, and 7.42-MeV transitions. The strengths for the ground-state and 1.63-MeV transitions were taken from Ref. 2, but were renormalized so that the value for the 6.72-MeV transition from that reference agreed with that from the present work. Also shown in Fig. 5 are the predictions of the SU(3) model (dashed lines). The predictions of the Nilsson model show fairly

good agreement with the data but only for values of δ between 0.1 and 0.2. This value of the deformation parameter is somewhat smaller than expected, perhaps implying that the simple Nilsson model is not adequate. The predictions of the SU(3) model also show fairly good agreement with the experimental results—within a factor of 2.

The lowest negative-parity bands expected to be excited in stripping are the $K^\pi=0^-$ and 1^- bands formed by the coupling of an odd particle in Nilsson orbit No. 14, $\frac{1}{2}^-[330]$ to the ^{19}F ground state. The $J^\pi=1^-$ state at 5.79 MeV is a good candidate for the first member of the $K^\pi=0^-$ band, which has only odd-spin members. The 7.17-MeV, $J^\pi=3^-$ state would then be the next member of this band. Both theoretical predictions show good agreement with the data for the 5.79-MeV 1^- member. The Nilsson model considerably overpredicts the strength of the 7.17-MeV 3^- transition, whereas the SU(3) model slightly underpredicts the strength. This transition is, however, very weak and the experimental spectroscopic strength may not be overly reliable.

The next positive-parity bands expected should be formed by the promotion of one nucleon to Nilsson orbit No. 7 $\frac{3}{2}^+[211]$, giving rise to $K^\pi=1^+$ and 2^+ bands. It is expected that the low-spin members of these bands will be strongly excited in both the $^{19}\text{F}(^3\text{He}, d)^{20}\text{Ne}$ and $^{21}\text{Ne}(^3\text{He}, \alpha)^{20}\text{Ne}$ reactions. The strong transition to the 9.859-MeV state makes it a candidate for being a member of one of these bands although the preferred spin of 3^+ leaves the location of the band head unknown. Further information on these rotational bands will be presented and discussed in a forthcoming paper on the $^{21}\text{Ne}(^3\text{He}, \alpha)^{20}\text{Ne}$ reaction.²²

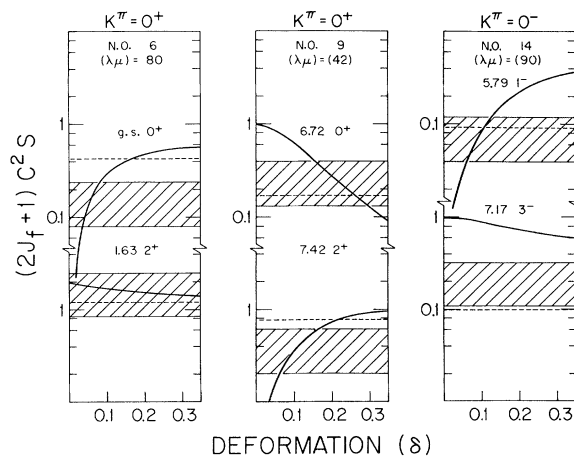


FIG. 6. Comparison between experimental spectroscopic strengths and the predictions of the Nilsson (solid lines) and SU(3) (dashed lines) models for three low-lying rotational bands in ^{20}Ne .

TABLE IV. Experimental and theoretical spectroscopic strengths for ^{20}Ne positive-parity states.

| J^π_N | Experiment | | Theory | | | |
|-----------|------------|-------------------|----------------|-------------|----------------|-------------|
| | E_x | | K- d s d^a | | F- p d s^b | |
| | (MeV) | $(2J_f+1)S$ | (MeV) | $(2J_f+1)S$ | (MeV) | $(2J_f+1)S$ |
| 0_1^+ | 0.00 | 0.34 ^c | 0.00 | 0.88 | 0.00 | 1.30 |
| 0_2^+ | 6.72 | 0.52 | 6.81 | 1.02 | 7.09 | 0.80 |
| 0_3^+ | 7.20 | 0.00 ^d | e | ... | 8.49 | 0.00 |
| 0_4^+ | ~8.3 | 0.13 | f | ... | f | ... |
| 2_1^+ | 1.63 | 3.47 ^c | 1.46 | 5.00 | 1.74 | 4.50 |
| 2_2^+ | 7.42 | 0.79 | 8.43 | 0.85 | 7.98 | 1.00 |
| 2_3^+ | 7.83 | 0.06 | e | ... | 8.57 | 0.00 |
| 3_1^+ | (9.86 | 2.37) | 10.69 | 3.99 | 10.07 | g |
| 3_2^+ | (11.55 | 1.00) | 11.90 | g | g | g |

^aReference 9.^bReference 11.^cReference 2, renormalized.^dLevel not observed.^eCore excited in this calculation.^fThought to be dominated by f - p shell configurations. Not included in the calculation.^gNot calculated.

In general, it is seen that the deformed models can give a reasonable description of the low-lying ^{20}Ne levels. The locations of higher-lying bands will provide a stringent test of this approach.

Shell model

Recently, large-basis shell-model calculations have been performed for nuclei in the $A=20$ region. As mentioned previously, the inevitable truncations in this type of calculation lead to an absence of certain classes of states. In particular the lowest $K^\pi=0^-$ band is not contained in any calculation. It is interesting, however, to compare the results of this type of calculation with the experimental results for those states expected to be well described within the truncated space. The calculations we shall consider are those of Refs. 9 and 11. The former assumed a closed ^{16}O core with the remaining four nucleons allowed to occupy the $1d_{5/2}$, $2s_{1/2}$, and $1d_{3/2}$ orbitals, whereas the latter allowed up to four holes in the $1p_{1/2}$ shell, with particles in the $2s_{1/2}$ and $1d_{5/2}$ orbitals (i.e. essentially a ^{12}C core). Both these calculations reproduce quite well the rotational bands in ^{20}Ne and the enhanced $E2$ transitions between the members of these bands. It is therefore to be hoped that these calculations will do equally well in predicting the single-nucleon spectroscopic strengths, which are more intimately related to this type of calculation than are the

TABLE V. Experimental and theoretical spectroscopic strengths for $T=1$ states in ^{20}Ne .

| J^π_N | Experiment | | Theory | | | |
|-----------|------------|--|--------------------|--|----------------|--|
| | E_x | | K- d s d^a | | F- p d s^b | |
| | (MeV) | $(2J_f+1)S$ | (MeV) | $(2J_f+1)S$ | (MeV) | $(2J_f+1)S$ |
| 2_1^+ | 10.26 | 0.07 | 10.26 ^c | 0.05 | 10.26 | 0.30 |
| 2_2^+ | 12.19 | 2.10 | 12.02 | 3.30 | 11.99 | 2.40 |
| 3_1^+ | 10.86 | 2.82 | 10.87 | 4.69 | 10.71 | 3.90 |
| 1_1^+ | (11.24) | $\begin{Bmatrix} 0.02 \\ 0.03 \end{Bmatrix}$ | 11.18 | $\begin{Bmatrix} 0.00 \\ 0.03 \end{Bmatrix}$ | 11.20 | $\begin{Bmatrix} 0.00 \\ 0.00 \end{Bmatrix}$ |
| 1_1^- | (11.24) | 0.02 | d | ... | 10.94 | ... |

^aReference 9.^bReference 11.^cFixed to agree with experimental energy.^dNot included in this calculation.

collective features. The experimental and theoretical excitation energies and spectroscopic strengths are compared in Tables IV and V. The over-all agreement is reasonably good, with the major discrepancy occurring for the ground-state transition. Recent investigations of the importance of second-order processes¹⁷ in the $^{19}\text{F}(^3\text{He}, d)^{20}\text{Ne}$ reaction show that the ground-state transition is strongly affected by these processes and that for other allowed transitions the effect is only of order 10% in the spectroscopic strengths.

The experimental spectroscopic strength of the 6.72-MeV 0^+ state is somewhat smaller than the predicted values. However, experimentally this model state is split between the 6.72- and 8.3-MeV 0^+ states. The summed strength of these two transitions is in reasonable agreement with both the predicted values.

For the 2^+ levels the agreement is excellent—the experimental and theoretical values agree to within 30%, which is the error usually associated with distorted-wave analyses.

The prediction of two 3^+ levels near 10 and 12 MeV, respectively, strengthens the belief that both the 9.86- and 11.55-MeV levels have $J^\pi=3^+$ as suggested by the I_p values and lack of width observed for these two states.

The $T=1$ levels show equally good agreement with the theoretical predictions, except that the F- p d s calculation grossly overestimates the strength of the ground-state transition.

We therefore see that the detailed shell-model calculations give reasonably good agreement with the experimental results for those classes of states contained in the truncated bases of the calculations. In fact, a calculation¹⁰ including all allowed configurations in the $1p_{1/2}$, $1d_{5/2}$, $2s_{1/2}$, and $1d_{3/2}$ or-

bitals does reproduce the positions and general features of the ^{20}Ne level scheme very well, although the exclusion of f - p shell orbitals is still a serious omission.

VI. CONCLUSIONS

The study of the $^{19}\text{F}(^3\text{He}, d)^{20}\text{Ne}$ reaction has enabled the assignment of several spins and parities. The locations of several $T=1$ levels have been determined or suggested. A comparison of the ex-

perimentally determined spectroscopic strengths with the predictions of both collective and microscopic models shows good agreement for the low-lying levels and the $T=1$ levels. The most serious discrepancy arises as a result of the necessary neglect of $1f$ - $2p$ shell orbitals in the shell-model calculations.

We acknowledge interesting and informative discussions with D. Cline, E. C. Halbert, J. B. McGrory, and J. Millener.

*Work supported by the National Science Foundation.

†Present address: Niels Bohr Institute, University of Copenhagen, Denmark.

¹A. E. Litherland, J. A. Kuehner, H. E. Gove, M. A. Clark, and E. Almqvist, *Phys. Rev. Lett.* **7**, 98 (1961).

²R. H. Siemssen, L. L. Lee, and D. Cline, *Phys. Rev.* **140**, B1258 (1965).

³J. P. Elliot and M. Harvey, *Proc. Roy. Soc. (Lond.)* **A272**, 557 (1963).

⁴M. Harvey, in *Advances in Nuclear Physics*, edited by M. Baranger and E. Vogt (Plenum, New York, 1968), Vol. 1, p. 67.

⁵J. A. Kuehner and E. Almqvist, *Can. J. Phys.* **45**, 1605 (1967).

⁶A. D. Panagiotou, H. E. Gove, and S. Harar, *Phys. Rev. C* **5**, 1995 (1972).

⁷R. W. Zurmühle, D. P. Balamuth, L. K. Fifield, and J. W. Noé, *Phys. Lett.* **44B**, 453 (1973).

⁸L. K. Fifield, R. W. Zurmühle, D. P. Balamuth, and J. W. Noé, *Phys. Rev. C* **8**, 2203 (1973).

⁹E. C. Halbert, J. B. McGrory, B. H. Wildenthal, and S. P. Pandya, in *Advances in Nuclear Physics*, edited by M. Baranger and E. Vogt (Plenum, New York, 1971), Vol. 4, p. 315.

¹⁰J. M. Irvine, G. S. Mani, V. Pucknell, A. Watt, and R. R. Whitehead, *Phys. Lett.* **44B**, 16 (1973).

¹¹J. B. McGrory and B. H. Wildenthal, *Phys. Rev. C* **7**, 974 (1973).

¹²F. Ajzenberg-Selove, *Nucl. Phys.* **A190**, 1 (1972).

¹³R. Jahr, *Phys. Rev.* **129**, 320 (1963).

¹⁴A. T. G. Ferguson, N. Gale, G. C. Harrison, and R. E. White, in *Proceedings of the Conference on Direct Interactions and Nuclear Reaction Mechanisms, Padua,*

Italy, 1962, edited by E. Clementel and C. Villi (Gordon and Breach, New York, 1963), p. 510.

¹⁵B. T. Lawergren, A. T. C. Ferguson, and G. C. Morrison, *Nucl. Phys.* **A108**, 325 (1968).

¹⁶R. C. Ritter, J. T. Parson, and D. L. Bernard, *Phys. Lett.* **28B**, 588 (1969).

¹⁷A. W. Obst and K. W. Kemper, *Phys. Rev. C* **8**, 1682 (1973).

¹⁸K. Abdo, Ph.D. Thesis, Florida State University, 1968 (unpublished).

¹⁹P. D. Kunz, unpublished.

²⁰H. T. Fortune, N. G. Puttaswamy, and J. L. Yntema, *Phys. Rev.* **185**, 1546 (1969).

²¹H. T. Fortune, T. J. Gray, W. Trost, and N. R. Fletcher, *Phys. Rev.* **179**, 1033 (1969).

²²R. R. Betts, H. T. Fortune, and R. Middleton, unpublished.

²³R. Middleton, J. D. Garrett, H. T. Fortune, and R. R. Betts, *J. Phys. (Paris) C* **6**, 39 (1971).

²⁴H. T. Fortune, R. Middleton, and R. R. Betts, *Phys. Rev. Lett.* **29**, 738 (1972).

²⁵H. T. Fortune, G. C. Morrison, R. C. Bearse, J. L. Yntema, and B. H. Wildenthal, *Phys. Rev. C* **6**, 21 (1972).

²⁶H. T. Fortune, R. R. Betts, and R. Middleton, *Phys. Rev. C* **10**, 1292 (1974).

²⁷G. F. Millington, J. R. Leslie, W. McLatchie, G. C. Ball, W. G. Davies, and J. S. Forster, *Nucl. Phys.* **A228**, 382 (1974).

²⁸J. John, J. P. Aldridge, and R. H. Davis, *Phys. Rev.* **181**, 1455 (1969).

²⁹G. R. Satchler, *Ann. Phys. (N.Y.)* **3**, 275 (1958).

³⁰B. E. Chi, *Nucl. Phys.* **83**, 97 (1966).